Acta Biomaterialia 10 (2014) 394–405

Contents lists available at ScienceDirect

Acta Biomaterialia

journal homepage: www.elsevier.com/locate/actabiomat

Bone healing and the effect of implant surface topography on osteoconduction in hyperglycemia

E. Ajami [a], E. Mahno [a], V.C. Mendes [a,b], S. Bell [a], R. Moineddin [c], J.E. Davies [a,b,*]

[a] Institute of Biomaterials and Biomedical Engineering, University of Toronto, 164 College Street, Toronto, Ontario M5S 3G9, Canada
[b] Dental Research Institute, Faculty of Dentistry, University of Toronto, 124 Edward Street, Toronto, Ontario M5G 1G6, Canada
[c] Department of Family and Community Medicine, Faculty of Medicine, University of Toronto, 263 McCaul Street, Toronto, Ontario M5T 1W7, Canada

ARTICLE INFO

Article history:
Received 25 June 2013
Received in revised form 12 September 2013
Accepted 18 September 2013
Available online 26 September 2013

Keywords:
Bone healing
Hyperglycemia
Implant
Surface topography

ABSTRACT

Dental implant failures that occur clinically for unknown reasons could be related to undiagnosed hyperglycemia. The exact mechanisms that underlie such failures are not known, but there is a general consensus that bone growth is compromised in hyperglycemia. Nevertheless, contradictory findings exist related to peri-implant bone healing in hyperglycemia. We hypothesized that hyperglycemia delays early bone healing by impeding osteoconduction, and that the compromised implant integration due to hyperglycemia could be abrogated by using nanotopographically complex implants. Thus we undertook two parallel experiments, an osteotomy model and a bone in-growth chamber model. The osteotomy model tracked temporal bone healing in the femora of euglycemic and hyperglycemic rats using micro computed tomography (microCT) analysis and histology. The bone in-growth chamber model used implant surfaces of either micro- or nanotopographical complexity and measured bone–implant contact (BIC) using backscattered electron imaging in both metabolic groups. Quantitative microCT analyses on bone volume, trabeculae number and trabeculae connectivity density provided clear evidence that bone healing, both reparative trabecular bone formation and remodeling, was delayed in hyperglycemia, and the reparative bone volume changed with time between metabolic groups. Furthermore, fluorochrome labeling showed evidently less mineralized bone in hyperglycemic than euglycemic animals. An increased probability of osteoconduction was seen on nano-compared with microtopographically complex surfaces, independent of metabolic group. The nanotopographically complex surfaces in hyperglycemia outperformed microtopographically complex surfaces in euglycemic animals. In conclusion, the compromised implant integration in hyperglycemia is abrogated by the addition of nanotopographical features to an underlying microtopographically complex implant surface.

1. Introduction

Diabetes mellitus has been described as a "group of metabolic disorders sharing the common underlying feature of hyperglycemia" [1], rather than a single disease entity. The International Diabetes Federation (IDF) reports an estimated 25 million diabetics in the USA, of which 7 million have not been diagnosed [2]. While the impact of diabetes can be seen in many different tissues and physiological systems, such as the kidneys, eyes, nerves and blood vessels, its effect on bone is notable [3,4], although not entirely understood.

Uncontrolled diabetes has been associated with an increased risk of dental implant failures [5–7], and it is possible that undiagnosed diabetes may be related to the 5% of dental implants that fail clinically for unknown reasons. Although the mechanisms that underlie such failures have not been clearly explained, the general consensus is that bone growth is compromised in hyperglycemia. The bone in hyperglycemic individuals is weaker and more fragile than healthy bone [4,8]. Affected individuals seem to have higher rates of osteoporotic fractures [9], slower wound healing [10], decreased skeletal growth during adolescence [11], and delayed or impaired fracture healing [12]. Nevertheless, the reports related to peri-implant bone formation and remodeling in hyperglycemia are contradictory, mostly due to obvious differences in animal models, implants employed, experimental procedures, and, most importantly, study time points.

Some reports show consistent decreases in bone volume adjacent to an implant [13], while others report an increase in the amount of bone [14]. Reports of decreased mechanical retention

* Corresponding author at: Institute of Biomaterials and Biomedical Engineering, University of Toronto, 164 College Street, Toronto, Ontario M5S 3G9, Canada. Tel.: +1 416 978 1471; fax: +1 416 946 5639.
E-mail addresses: jed.davies@utoronto.ca, jed@verypowerfulbiology.com (J.E. Davies).

1742-7061/$ - see front matter © 2013 Acta Materialia Inc. Published by Elsevier Ltd. All rights reserved.
http://dx.doi.org/10.1016/j.actbio.2013.09.020

of implants [15] and bone–implant contact (BIC) [14,16–18], which is the product of osteoconduction and de novo bone formation, provide support for the notion of compromised peri-implant healing in diabetic subjects, yet no mechanistic explanations exist for such differences. We believe that chronic hyperglycemia has an impact on the early stages of peri-implant healing, specifically osteoconduction and de novo bone formation, which consequently affects long-term endosseous implant stability. This could lead to an increased number of implant failures in the undiagnosed hyperglycemic population compared with a truly healthy population.

In the present study we monitored the effects of hyperglycemia on early bone healing and, specifically, tested the effect of hyperglycemia on osteoconduction, in the presence of candidate implant surfaces, using a previously established model [19]. We hypothesize that hyperglycemia could delay early bone healing by impeding osteoconduction. Since osteoconduction, together with bone formation, results in contact osteogenesis, and since nanotopographically complex implant surfaces have previously been shown to accelerate osteoconduction [19], we also hypothesize that compromised implant integration due to hyperglycemia could be abrogated by using nanotopographically complex endosseous implants. To address our hypotheses we undertook two parallel experiments. In the first, an osteotomy model, we created femoral drill holes in both hyperglycemic and healthy rats and tracked bone healing with time by micro computed tomography (microCT) and histology. In the second, an implant model, we measured BIC in both hyperglycemic and healthy rats using custom bone in-growth chambers modified with either micro- or nanotopographically complex surfaces.

2. Materials and methods

2.1. Design of "T-plant" bone in-growth chambers

200 titanium (commercially pure grade IV) bone in-growth chambers, termed T-plants (Fig. 1A), were custom fabricated by Biomet 3i (Palm Beach Gardens, FL) for this study. The implants were machined in two modular parts and then assembled. The external dimensions of each T-plant are approximately $5 \times 3 \times 2$ mm (height × width × depth), and the internal chamber has dimensions of $3 \times 3 \times 1$ mm (height × width × depth) (Fig. 1B).

Four different surface treatments were applied to generate micro- and nanotopographically complex surface designs on 200 implants. Initially all chambers were acid etched by a dual acid etch (DAE) method in 8% HF solution followed by 78% H_2SO_4/3% HCl solution (wt.%). No further modification was made to 50 implants (DAE group). Of the remaining implants, 50 implants were further etched in 3% KOH/17% H_2O_2 (wt.%) at 52 °C for 1 min (MAE group), while another 50 were etched in 22% KOH at 60 °C for 65 min (NAT group). Both groups were then treated with HNO_3 at 60 °C for 10 min, rinsed in water and dried in an oven at 110 °C. The remaining 50 implants were modified by the deposition of discrete crystalline calcium phosphate nanocrystals (DCD group). For the DCD treatment implants were dipped in an alcohol-based suspension containing 1% nanocrystals of stoichiometric hydroxyapatite (20–100 nm in size, ⩾95% crystalline) at room temperature and dried in an oven at 100 °C.

Thus a total of four groups, each containing 50 samples, were generated.

2.2. Characterization of candidate implant surfaces

2.2.1. Surface roughness

Surface roughness analysis was performed using an optical interferometer (MicroXAM-100, ADE Phase Shift, KLA-Tencor, Milpitas, CA). The data was obtained at 312.5× magnification, over a 52,400 mm^2 implant area. A 50 mm Gaussian filter and inverse fast Fourier transformation were employed.

2.2.2. Field emission scanning electron microscopy (FE-SEM)

Two additional T-plants from each surface group were opened by carefully prizing the two walls of the chambers apart with a scalpel blade. This procedure was done with extreme caution so as not to damage or contaminate the internal walls of the chambers. The internal surface topography of the chamber walls was observed by FE-SEM (Hitachi S-5200, Japan) at an accelerating voltage of 5 keV and increasing magnification (up to 100,000×) at the Centre for Nanostructure Imaging, University of Toronto, without coating with an electron-conducting medium.

2.3. Animals

The experimental protocol was approved by the Ethics Committee of Animal Research at the University of Toronto. 180 Young male Wistar rats (200–250 g, Charles River Laboratories, Canada) were housed at the animal facility of the Faculty of Dentistry, University of Toronto. Animals were allowed to adapt for 1 week prior to commencement of the study. They had free access to rat chow and water throughout the study. 80 Animals were used for the osteotomy model and 100 for the implantation model. In each study the animals were divided into two metabolic groups, hyperglycemic (H) and healthy control (C). Thus the final animal groups

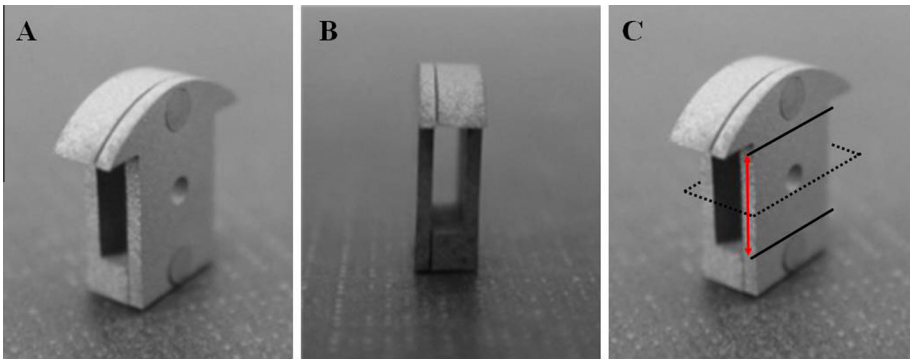

Fig. 1. (A) View of the bone in-growth chamber, which is assembled in modular parts and has the shape of a "T". The external dimensions of the T-plant chamber are 5 (H) × 3 (W) × 2 (D) mm. (B) Side view of the T-plant showing the chamber into which bone grows. The internal dimensions are 3 (H) × 3 (W) × 1 (D) mm. (C) The plane of grinding, which is shown dotted, was along the long axis of the femur to produce a cross-section showing both walls of the T-plant chamber. The double arrow shows the area that accommodated eight cross-sectional layers with 250 ± 50 μm intervals.